Lineage tracing of the bivalve shell field with special interest in the descendants of the 2d blastomere

doi: 10.1098/rsbl.2015.1055

Lineage tracing of the bivalve shell field with special interest in the descendants of the 2d blastomere

Masakuni Mohri, Naoki Hashimoto and Hiroshi Wada*

Graduate School of Life and Environmental Sciences, University of Tsukuba, Tsukuba 305-8572, Japan

*Author for Correspondence;

Tel&Fax:+81-29-853-4671

e-mail:hwada@biol.tsukuba.ac.jp

Abstract

By evolving bilaterally separated shell plates, bivalves acquired a unique body plan in which their soft tissues are completely protected by hard shell plates. In this unique body plan, mobility between the separated shell plates is provided by novel structures such as a ligament and adductor muscles. As a first step toward understanding how the bivalve body plan was established, we investigated the development of the separated shell plates and ligament. Over 100 years ago it was hypothesized that the development of separated shell plates is tightly linked with the unique cell cleavage (division) pattern of bivalves during development, wherein each bilateral daughter cell of the 2d descendant, $2d^{1121}$, develops into one of the bilateral shell fields. In the present study we tested this hypothesis by tracing the cell lineages of the Japanese purple mussel *Septifer virgatus*. Although the shell fields were found to be exclusively derived from the bilateral descendant cells of 2d: $2d^{11211}$ and $2d^{11212}$, the descendants of these cells were not restricted to shell fields alone, nor were they confined to the left or right side of the shell field based on their lineage. Our study demonstrated that ligament cells are also derived from $2d^{11211}$ and $2d^{11212}$ indicating that the ligament cells

35 emerged as a subpopulation of shell field cells. This also suggests that the
36 establishment of the novel developmental system for the ligament cells was
37 critical for the evolution of the unique bodyplan of bivalves.
38

1.INTRODUCTION

Molluscs share several characteristic features, such as calcareous shells (or spicules) and a muscular foot. However, their body plans are highly variable, as demonstrated by the differences between the worm-like, shell-less Aplacophora and the highly motile Cephalopoda. With the development of bilaterally separated shell plates, bivalves evolved a unique body plan in which their soft tissue is completely protected by hard shell plates. The muscle system was rearranged to accommodate the evolution of this shell plate morphology, resulting in another evolutionary novelty, the adductor muscle, which controls the opening and closing of the shell plates. Determining how this unique bivalve body plan was achieved through the coordinated evolution of shell plate morphology and muscles is challenging. To address this question we first investigated how the bilaterally separated shell plates developed through the modification of shell development.

Over 100 years ago Lillie and Meisenheimer [1, 2] reported a pattern of spiral cleavage in bivalves. Most molluscan species exhibit spiral cleavage wherein the animal blastomeres are smaller than the vegetal blastomeres.

However, the dorsal vegetal blastomeres (1D) produce a larger animal blastomere (2d) in bivalves from the eight-cell stage to the 16-cell stage[3, 4]. This animal blastomere is thought to be the precursor of the shell field cells, which underlie shell plates[1, 2]. After four rounds of asymmetric cleavage, the largest blastomere ($2d^{1121}$) exhibits bilateral cleavage (Figure 1a-e), and the bilateral daughter cells were suggested to differentiate into the left and right shell field cells of their respective side[1]. This hypothesis suggests that development of the novel shell plate morphology was driven by a modification of the early cleavage pattern. However, it was based solely on microscopic observations and experimental validation is required through direct cell lineage tracing.

It is also notable that bivalves show a stereotypic pattern of spiral cleavage prior to the occurrence of bilateral cleavage. The largest blastomere, 2d, undergoes four rounds of asymmetric spiral cleavage prior to the bilateral cell division (Figure 1a-e). The first two rounds of asymmetric cleavage give rise to two smaller vegetal blastomeres, $2d^{2}$ and $2d^{12}$, and a larger animal blastomere, $2d^{11}$ (Figure 1a-b). When $2d^{11}$ divides the polarity is reversed, and a smaller animal blastomere ($2d^{111}$) and a larger vegetal blastomere ($2d^{112}$) are generated

74 (Figure 1c). The cell size polarity is again reversed during the next cleavage of
75 $2d^{112}$, yielding a smaller vegetal blastomere ($2d^{1122}$) and a larger animal
76 blastomere ($2d^{1121}$; Figure 1e). Blastomere $2d^{1121}$ then divides symmetrically to
77 produce a left ($2d^{11211}$) and right daughter ($2d^{11212}$)(Figure 1e).
78 In the present study we investigated how this series of cleavages is
79 linked with the development of the unique morphology of bivalves. Focusing on
80 the shell field precursors in bivalve embryos we traced the cell lineages of the
81 early blastomeres with a fluorescent photoconversion technique using Kaede
82 fluorescent protein[5].
83
84 **2.MATERIALS AND METHODS**
85 Adult specimens of the Japanese purple mussel *Septifer virgatus* (Wiegmann,
86 1837) were collected in Tsuyazaki, Fukuoka Prefecture, Japan. Induction of
87 spawning and in vitro fertilization were performed as described in [4]. The
88 handedness of spiral cleavage was unexpectedly reversed in the eggs from
89 Tsuyazaki individuals compared with those from Kashima described in
90 [4](dextral in Kashima [4] and sinistral in Tsuyazaki: this study), and we

91 confirmed that the direction of the spiral cleavage was reversed for all cleavages
92 up to the bilateral cleavage of $2d^{1121}$ for all specimens examined (Figure 1a-e,
93 Table 1). This polymorphism in the handedness of spiral cleavage has been
94 reported in another bivalve species *Dreissena polymorpha*[6].
95 mRNA for Kaede was transcribed from a pBluescript RN3 vector[7], and
96 Kaede mRNA (3 μg/μl) was injected into fertilized eggs.
97 Kaede fluorescence can be irreversibly converted from green to red by
98 irradiation with ultraviolet light. Photoconversion was performed using a
99 confocal laser scanning microscope (CLSM. Zeiss LSM710, Germany) at a 405 nm
100 wavelength. The laser was applied until we confirmed that sufficient
101 photoconversion was induced. Among photoconverted embryos, about 20%
102 showed abnormal morphology at the trochophore stage and were excluded from
103 our analysis. Swimming larvae were immobilized prior to observation by fixing
104 with 4% paraformaldehyde and observed by CLSM. The fluorescent signal could
105 be observed up to 10 h after fixation. It should be noted that some converted cells
106 appeared yellowish because unconverted green Kaede protein was translated

from the injected mRNA even after photoconversion. Unmerged fluorescent signals are shown in Figure S1.

3.RESULTS

To confirm that 2d blastomeres contribute shell field precursors, 2d blastomeres were photoconverted at the nine-cell stage. Following photoconversion of a 2d blastomere, the converted signal was widely detected in the dorsal region of the post-trochal epidermis (Figure 2a-c). Importantly, all of the shell field cells were labeled (Figure 2b, Table 1), indicating that the shell field cells were solely derived from 2d descendants.

Prior to the occurrence of bilateral cleavage, 2d blastomeres undergo four rounds of asymmetric cleavage to produce four micromeres (Figure 1a-d). These micromeres were photoconverted after the bilateral cleavage of $2d^{1121}$ because each blastomere is most easily identified at this stage of development.

At this stage, derivatives of $2d^{2}$ have already undergone two rounds of cell division. We photoconverted all of the derivatives of $2d^{2}$ (Figure 2j). The converted signal was detected in the left side of both the anterior and posterior of

124 the post-trochal epidermis in these larvae. Importantly, however, the signal was
125 not detected in the shell field (Figure 2k, Table 1).

126 When $2d^{12}$ was photoconverted, the signal was observed on the right side
127 of the anterior of the post-trochal epidermis, but no signal was detected in the
128 shell field (Figure 2l-m, Table 1).

129 When the $2d^{111}$ micromere was photoconverted, the signal was detected
130 in the anterior dorsal midline of the post-trochal epidermis (Figure 2o-p, Table 1).
131 When $2d^{1122}$ was labeled, the signal was detected in the posterior epidermis
132 (Figure 2q-r, Table 1). No signal was detected in the shell field in either case ($2d^{111}$
133 or $2d^{1122}$).

134 We then photoconverted each bilateral daughter of $2d^{1121}$ to determine
135 whether the bilateral shell fields differentiate according to the bilateral cleavage
136 of $2d^{1121}$. When $2d^{11211}$ (the left side daughter of $2d^{1121}$) was photoconverted, the
137 signal was detected not only in the shell field, but also in the surrounding
138 epidermis (Figure 2d-f). Thus, even at this stage the developmental outcome is
139 not restricted to the shell field cells. Importantly, the signal was detected not only
140 in the left side of the shell field, but also in the right side (Figure 2e, Table 1).

Interestingly, the signal was biased toward the left posterior in all larvae. Similarly, when $2d^{11212}$ (the right side daughter of $2d^{1121}$) was photoconverted, the signal was observed in both the shell field and the surrounding epidermis (Figure 2g-i, Table 1). The signal in the shell field was biased toward the right anterior of the shell fields in all larvae.

Bivalve shell fields are bilaterally separated by ligament cells that develop along the dorsal midline (Fig. 1f, g, [3]). Differentiation of the ligament cells is clearly visible by specific upregulation of the *chitin synthase* (*cs*) gene during the trochophore stage[8]. Photoconversion indicated that all of the shell field cells are derived either from $2d^{11211}$ or $2d^{11212}$. Based on *dpp* expression noted in oyster embryos, Kin et al.[3] suggested previously that ligament cells are derived from the descendants of $1d^{12}$ and $2d^{2}$. Thus, we examined any possible contribution from the 1d cell lineage, and found that 1d develops into the anterior epidermis, including the prototroch (Figure S2, Table 1), but not into shell field. Thus we concluded that the ligament cells are only derived from $2d^{11211}$ and $2d^{11212}$.

4. DISCUSSION

In the present study we found that all shell field precursors are derived from $2d^{1121}$, although the developmental fate of $2d^{1121}$ is not restricted to the shell field cells alone. Importantly, the bilateral shell fields were not derived exclusively from the daughter cells of $2d^{1121}$ of each respective side. Instead, the derivatives of the daughter blastomeres contributed to both sides of the shell field by spreading across the midline (Figure 1f, g, 2e,h). Thus, our results did not support the classical hypothesis that the bilaterally separated shell plates of bivalves are derived from bilateral descendants of 2d[1]. It is notable that descendants of the 2d blastomere also show bilateral cell division in gastropods, as well as in annelids (e.g., [9-13]), and together with 4d, 2d was shown to demonstrate organizing activity in annelids[14]. So it is likely that the bilateral cell division of 2d descendants was established much earlier than the emergence of bivalves, possibly for the establishment of the bilateral body plan from the spiral cleavage[15]. The bilateral shell plates, however, might have evolved irrespective of bilateral cleavage.

The innovation of ligament cells in the dorsal midline of the shell field is critical for the unique body plan of bivalves[16]. Our lineage tracing indicates that ligament cells differentiate from the $2d^{1121}$ lineage of cells just like other shell field cells (Figure 1f, g, 2d-i), indicating that the ligament cells emerged as a subpopulation of shell field cells. The ligament cells are specifically marked by the upregulation of *cs* [8], and the expression of *dpp* earlier than *cs* [3]. Prior to shell field invagination, *dpp* is also expressed in cells abutting the shell field midline, both anteriorly and posteriorly [3]. Although we demonstrated that these *dpp* positive cells ($1d^{12}$ and $2d^{2}$) do not differentiate into either shell field cells or ligament cells, it is still possible that *dpp* plays an inductive role in ligament differentiation. Functional studies of bivalve *dpp* may advance our understanding of the evolution of the unique bivalve body plan.

Innovation of the ligament provided mobility between the separated shell plates of bivalves, and thus it may have accompanied the evolution of adductor muscles to open and close the shells. Elucidation of the developmental mechanism of ligament cells may provide a clue to understanding how the

innovation of the ligament and that of adductor muscles are linked during evolution.

Ethics: Research was carried out according to the university's guideline.

Data accessibility: The datasets supporting this article have been uploaded as part of the supplementary material.

Author's contribution: All authors contributed to the design of the study, collection of data and writing of the article. All authors approve the final version of this manuscript and agree to be held accountable for all aspects of the work performed.

Competing interests: We declare we have no competing interests.

Acknowledgement: We thank Yoshihisa Kurita for providing us purple mussesls, and also for sharing unpublished results.

Funding: NH was supported as JSPS pre-doctoral research fellow.

References

[1] Lillie, F.R. 1895 The embryology of the Unionidae. A study in cell lineage. *J. Morphol.* **10**, 1-100.

[2] Meisenheimer, J. 1901 Entwicklungsgeschichte von *Dreissensia polymorpha* Pall. *Zeitschrift f. wissensch. Zoologie* **69**, 1-137.

211 [3] Kin, K., Kakoi, S. & Wada, H. 2009 A novel role for *dpp* in the shaping of
212 bivalve shells revealed in a conserved molluscan developmental progaram. *Dev.*
213 *Biol.* **329**, 152-166.
214 [4] Kurita, Y., Deguchi, R. & Wada, H. 2009 Early development and cleavage
215 pattern of the Japanese purple mussel, *Septifer virgatus*. *Zool. Sci.* **26**,
216 814-820.
217 [5] Ando, R., Hama, H., Yamamoto-Hino, M., Mizuno, H. & Miyawaki, A. 2002 An
218 optical marker based on the UV-induced green-to-red photoconversion of a
219 fluorescent protein. *Proc. Natl. Acad. Sci. USA* **99**, 12651-12656.
220 [6] Luetjens, C.M. & Dorrestejin, A.W. 1995 Multiple, alternative cleavage
221 patterns precede uniform larval morphology during normal develoment of
222 *Dreissena polymorpha* (mollusca, Lamellibranchia). *Roux's Arch. Dev. Biol.* **205**,
223 138-149.
224 [7] Lemaire, P., Garrett, N. & Gurdon, J.B. 1995 Expression cloning of *Siamois*, a
225 *Xenopus* homeobox gene expressed in dorsal vegetal cells of blastulae and able
226 to induce a complete secondary axis. *Cell* **81**, 85-94.
227 [8] Hashimoto, N., Kurita, Y., Murakami, K. & Wada, H. 2014 Cleavage pattern
228 and development of isolated D blastomeres in bivalves. *J. Exp. Zool. (Mol. Dev.*
229 *Evol.)* **324B**, 13-21.
230 [9] Conklin, E.G. 1897 The embryology of *Crepidula*. *J. Morphol.* **13**, 3-209.
231 [10] Schneider, S.Q. & Bowerman, B. 2007 ß-catenin asymmetries after all
232 animal/vegetal-oriented cell divisions in *Platynereis dumeriliiembryos* mediate
233 binary cell-fate specification. *Dev. Cell* **13**, 73-86.

234 [11] Meyer, N.P. & Seaver, E. 2010 Cell lineage and fate map of the primary
235 somatoblast of the polychaete annelid *Captella teleta*. *Integr. Comp. Biol.* **50**,
236 756-767.
237 [12] Chan, X.Y. & Lambert, J.D. 2014 Development of blastomere clones in the
238 *Ilyanassa* embryo: transformation of the spiralian blastula into the larval body
239 plan. *Dev. Genes Evol.* **224**, 159-174.
240 [13] Lyons, D.C., Perry, K.J. & Henry, J.Q. 2015 Spiralian gastrulation: germ
241 layer formation, morphogenesis, and fate of the blastopore in the slipper snail
242 *Crepidula fornicata*. *EvoDevo* **6**, 24.
243 [14] Nakamoto, A., Nagy, L.M. & Shimizu, T. 2011 Secondary embryonic axis
244 formation by transplantation of D quadrant micromeres in an oligochaete
245 annelid. *Development* **138**, 283-290.
246 [15] Lyons, D.C., Perry, K.J., Lesoway, M.P. & Henry, J.Q. 2012 Cleavage pattern
247 and fate map of the mesentoblast, 4d, in the gastropod *Crepidula*: a hallmark
248 of spiralian development. *EvoDevo* **3**, 21.
249 [16] Owen, G., Trueman, E.R. & Younge, C.M. 1953 The ligament in the
250 Lamellibranchia. *Nature* **171**, 73-75.
251
252

Figure legends

Figure 1. Schematic illustration of the cleavage pattern and cell lineage mapping of 2d descendants.

(a-e)Schematic illustration of the cleavage pattern of 2d descendants. (f)Summary of the cell lineage mapping of the 2d descendants in trochophore larva. Dorsal views, anterior to the top.(g) Tree diagram of the cell lineage and developmental fate of 2d descendants.

Figure 2. Cell lineage tracing of 2d and descendant blastomeres.

(a-c)Cell lineage of 2d. Kaede was converted at 9 cell stage (a: view from right side), and the fate of 2d was observed at trochophore stage (b-c). (d-r)Cell lineage of $2d^{11211}$(d-f), $2d^{11212}$ (g-i), $2d^{2}$(j-k), $2d^{12}$ (l-m), $2d^{111}$(o-p) and $2d^{1122}$(q-r). Noted that some converted cells appeared yellowish because unconverted green Kaede protein was translated from the injected mRNA even after photoconversion. Shell field boundary is indicated by broken line. Anterior to the top except for (o) in which ventral to the top. Scale bars: 50μm.

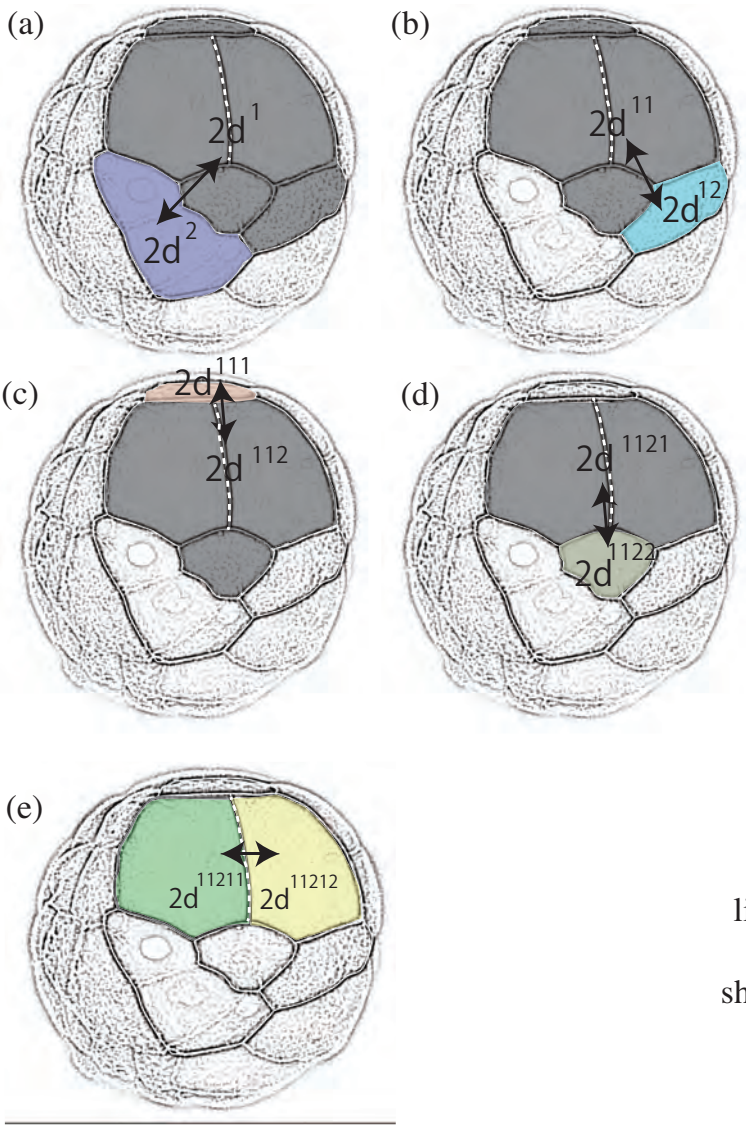
(a)
2d 1
2d 2
(b)
2d 11
2d 12
(c)
2d 111
2d 112
(d)
2d 1121
2d 1122
(e)
2d 11211
2d 11212

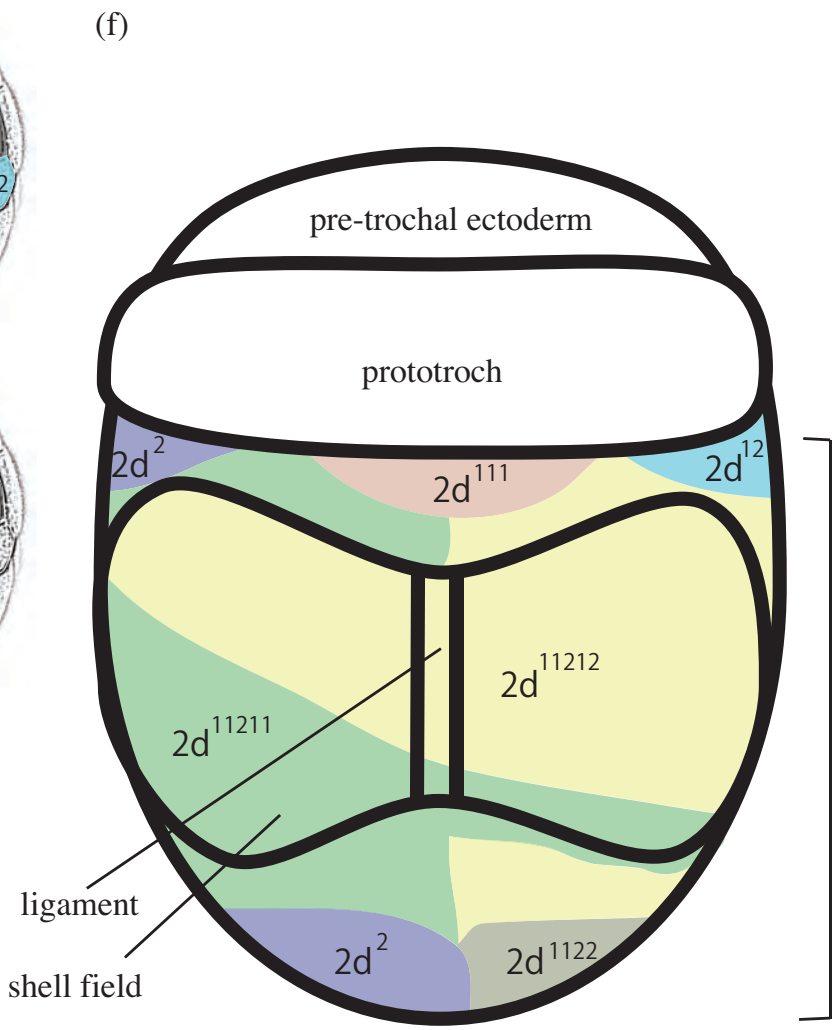
(f)
pre-trochal ectoderm
prototroch
2d 2
2d 111
2d 12
2d 11212
2d 11211
ligament
shell field
2d 2
2d 1122
post-trochal ectoderm

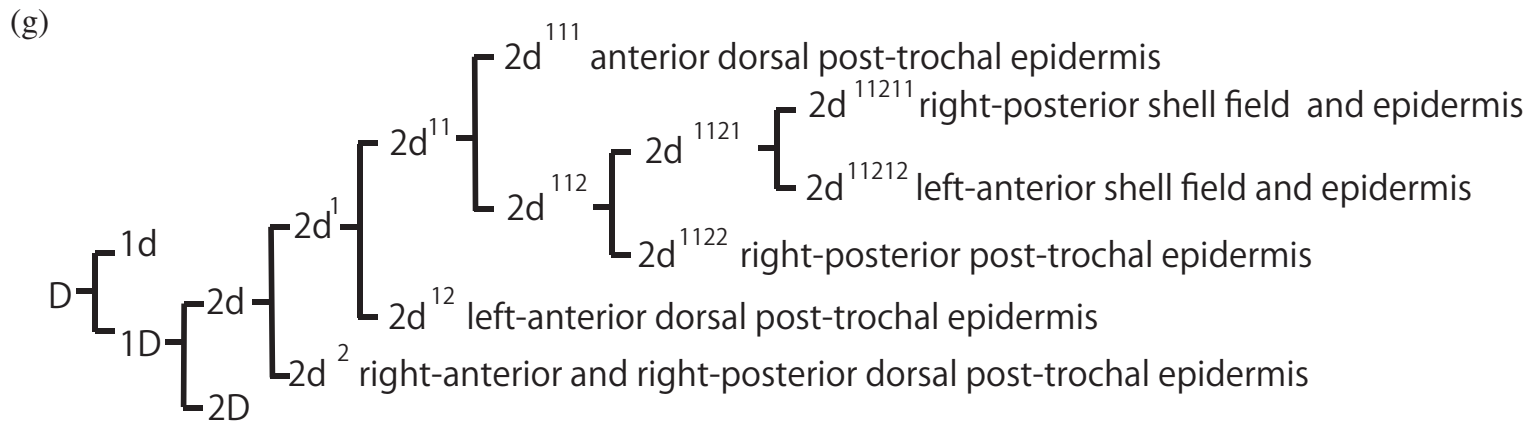
(g)
2d 111 anterior dorsal post-trochal epidermis
2d 11211 right-posterior shell field and epidermis
2d 11212 left-anterior shell field and epidermis
2d 1122 right-posterior post-trochal epidermis
2d 12 left-anterior dorsal post-trochal epidermis
2d 2 right-anterior and right-posterior dorsal post-trochal epidermis
2d 11
2d 112
2d 1121
2d 1
2d
1d
D
1D
2D

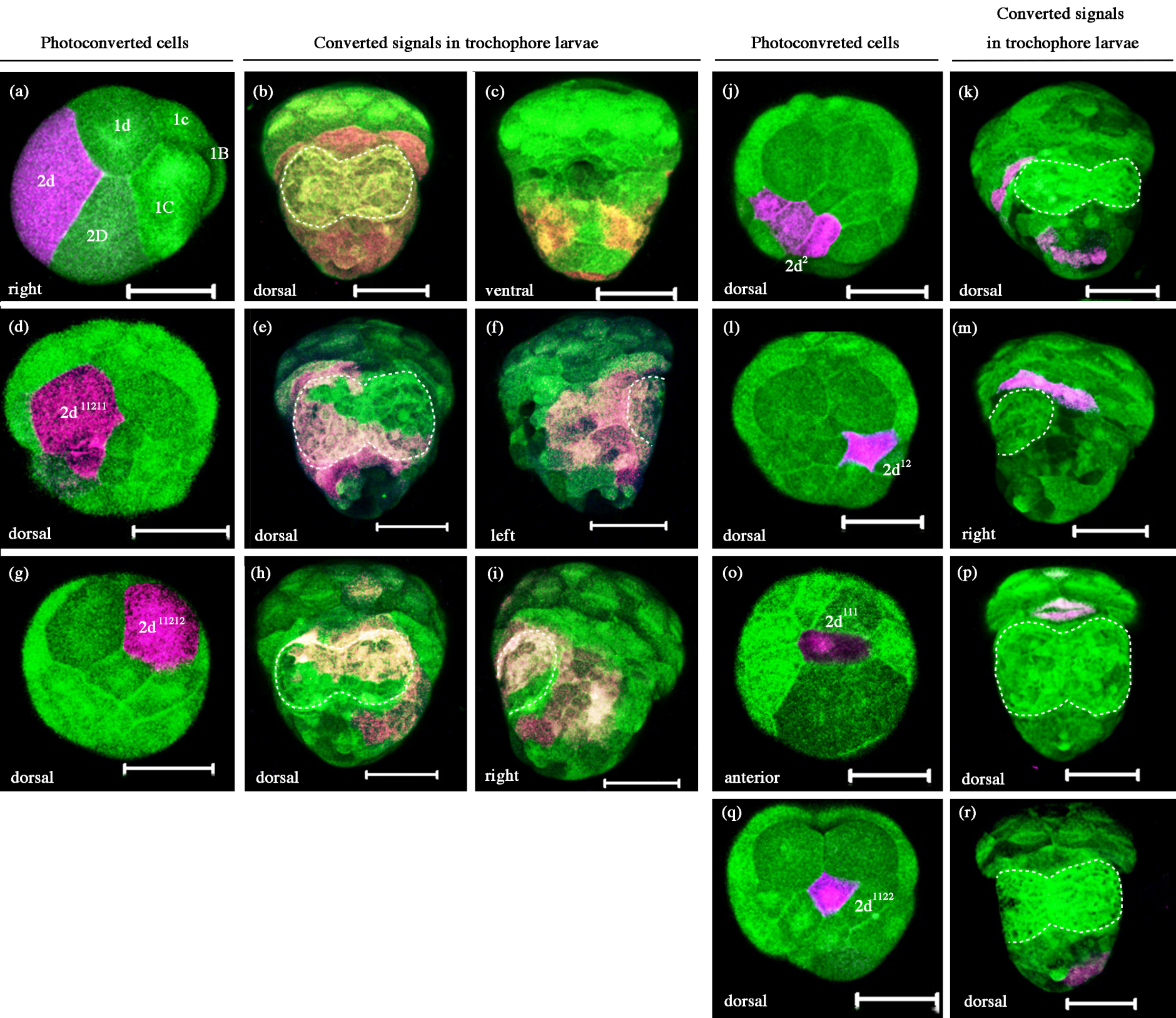
Photoconverted cells
Converted signals in trochophore larvae
Photoconvreted cells
Converted signals
in trochophore larvae
(a)
1d
1c
1B
2d
1C
2D
right
(b)
dorsal
(c)
ventral
(j)
2d2
dorsal
(k)
dorsal
(d)
2d11211
dorsal
(e)
dorsal
(f)
left
(l)
2d12
dorsal
(m)
right
(g)
2d11212
dorsal
(h)
dorsal
(i)
right
(o)
2d111
anterior
(p)
dorsal
(q)
2d1122
dorsal
(r)
dorsal

Table 1. Cell lineage of 2d descendants

photoconverted cells	developmental fate at trochophore stage	no. larvae showing the fate / no. embryos observed	Figure
2d	dorsal post-trochal epidermis and shell field	4/4	2a-c
2d2	right-anterior and right-posterior dorsal post-trochal epidermis	8/8	2j-k
2d12	left-anterior dorsal post-trochal epidermis	6/6	2l-m
2d111	anterior dorsal post-trochal epidermis	6/6	2o-p
2d1122	right-posterior post-trochal epidermis	7/7	2q-r
2d11211	right-posterior shell field and ligament right-anterior and posterior dorsal post-trochal epidermis	8/8	2d-f
2d11212	left-anterior shell field and ligament left-anterior and posterior dorsal post-trochal epidermis	9/9	2g-i
1d	prototroch and pre-trochal epidermis	4/4	S1